Oxidative potential of logwood and pellet burning particles assessed by a novel profluorescent nitroxide probe

B. Miljevic[1,5], M.F. Heringa[4], A. Keller[2], N.K. Meyer[2#], J. Good[3], A. Lauber[3], P.F. DeCarlo[4], K.E. Fairfull-Smith[5], T. Nussbaumer[3], H. Burtscher[2], A.S.H. Prevot[4], U. Baltensperger[4], S.E.Bottle[5] and Z.D. Ristovski[1*]

[1]*International Laboratory for Air Quality and Health, Queensland University of Technology, Brisbane, Australia*

[2]*Institute for Aerosol and Sensor Technology, University of Applied Sciences, Windisch, Switzerland*

[3]*Lucerne School of Engineering and Architecture, Lucerne University of Applied Sciences and Arts, Horw, Switzerland*

[4]*Laboratory for Atmospheric Chemistry, Paul Scherrer Institut, Villigen, Switzerland*

[5]*ARC Centre of Excellence for Free Radical Chemistry and Biotechnology, Queensland University of Technology, Brisbane, Australia*

[#]*now at Laboratory for Energy Systems Analysis, Paul Scherrer Institut, Villigen, Switzerland*

[*]Corresponding author: Z.D. Ristovski

Email address: z.ristovski@qut.edu.au

Telephone number: +617 3138 1129

Fax number:+617 3138 9079

Abstract

This study reports the potential toxicological impact of particles produced during biomass combustion by an automatic pellet boiler and a traditional logwood stove under various combustion conditions using a novel profluorescent nitroxide probe BPEAnit. This probe is weakly fluorescent, but yields strong fluorescence emission upon radical trapping or redox activity. Samples were collected by bubbling aerosol through an impinger containing BPEAnit solution, followed by fluorescence measurement. The fluorescence of BPEAnit was measured for particles produced during various combustion phases, at the beginning of burning (cold start), stable combustion after refilling with the fuel (warm start) and poor burning conditions. For particles produced by the logwood stove under cold-start conditions significantly higher amounts of reactive species per unit of particulate mass were observed compared to emissions produced during a warm start. In addition, sampling of logwood burning emissions after passing through a thermodenuder at 250^{o}C resulted in an 80-100% reduction of the fluorescence signal of BPEAnit probe, indicating that the majority of reactive species were semivolatile. Moreover, the amount of reactive species showed a strong correlation with the amount of particulate organic material. This indicates the importance of semivolatile organics in particle-related toxicity. Particle emissions from the pellet boiler, although of similar mass concentration, were not observed to lead to an increase in fluorescence signal during any of the combustion phases.

Introduction

Due to increasing energy demand, and recognition of climatic effects from fossil fuel combustion, there is need for alternative energy sources. Within that scope biomass combustion is regaining importance as being a source of renewable energy. Biomass combustion for heating purposes is common in countries with a colder climate, where it presents a significant source of both gaseous and particulate pollutants affecting in that way local air quality and health (*1, 2*). While there are many epidemiological and toxicological studies linking particles, in general, with various adverse health outcomes (e.g., (*3, 4*)), evaluations of potential health impacts of particles produced during biomass combustion are somewhat limited. However, several studies have indicated that exposure to biomass combustion particulate matter (PM) leads to reactive oxygen species (ROS) generation, DNA damage, lipid peroxidation and release of proinflammatory cytokines in lung cells (*5-8*). A review on the health effects of wood smoke by Naeher et al. (*9*) points out that although there is enough evidence linking biomass smoke exposure with adverse health effects, there is insufficient amount of data to judge the relative toxicity of biomass combustion particulate emissions compared to particles produced from other combustion sources. Kocbach et al. (*10*) have reported that wood smoke and traffic-derived particles induce a similar proinflammatory response in monocytes, although with different response patterns. However, a recent review article by Kocbach Bolling et al. (*11*) emphasizes a need to explore more how combustion conditions and the type of fuel and combustion appliance influence the toxicological potential of the emitted particles.

The underlying mechanisms for particle-related health effects are still not entirely understood, but a widely accepted hypothesis for the adverse health outcomes induced by particles is that they are able to generate ROS and, thus, induce oxidative stress within affected cells (*12, 13*). In addition, several studies have shown that particles may also contain ROS, presenting a direct cause of oxidative stress (*14-16*). Therefore, the amount of particle-

related ROS is an important parameter in assessing the potential toxicological impact of particulate matter.

The aim of this study was to assess the potential of particles produced by an automatic pellet boiler and a logwood stove to cause oxidative stress as measured by a novel profluorescent nitroxide probe, BPEAnit. BPEAnit and other profluorescent nitroxides are weakly fluorescent compounds, but exhibit strong fluorescence emission upon radical trapping or redox activity (*17-19*). Recently, BPEAnit was applied in the assessment of oxidative potential of combustion-derived particles, namely, cigarette smoke and diesel exhaust particles (*20, 21*), where the amount of BPEAnit converted to a fluorescent product served as a measure of oxidative activity of PM. However, it should be noted that, as being an abiotic assay, BPEAnit method can measure only PM's inherent oxidative potential, it cannot reflect the total oxidative activity that requires the PM interaction with the cellular matrix to be considered.

In many developed countries where biomass combustion for heating purposes is widely in use, automatic pellet boilers and traditional wood stoves are common residential combustion appliances. In general, automatic appliances exhibit well regulated combustion conditions with higher combustion efficiencies and thus decreased emissions of products of incomplete combustion. For example, Johansson et al. (*22*) reported that mass concentrations of particulate matter were up to 180 times larger for an old-type wood boiler compared to a modern wood pellet burner. Furthermore, under ideal operating conditions, the automatic burners were found to emit particles dominated by alkali metal salts (KCl, K_2SO_4) (*23*). Traditional wood stoves, on the other hand, are manually fed with fuel, experiencing less controlled combustion conditions resulting in highly variable emissions with higher relative fractions of organic species and soot compared to the automatic burners. Several studies have

reported that the organic fraction can contribute in excess of 50% of the total particle mass (*24*, *25*).

Experimental

Wood burners. The traditional wood stove used in this study (Carena, Tiba, Switzerland) had a nominal power output of 8 kW and was batch fired with beech logs (moisture content 20%). The fire was ignited from the top (ignition of small pieces of wood which were put on top of the logs). This type of ignition has been observed to reduce total PM emissions by 50 – 80% compared to traditional bottom-up ignition *(26)*. In Switzerland, the top-down burning method has been proposed as a method for reducing the contributions of particulate matter emissions from traditional wood stoves to national emission inventories. For the majority of measurements involving logwood, the fuel was combusted in four sequential batches, each batch having a fuel load of 2-3 kg. Each complete combustion cycle consisted of a cold start (start-up and stable burning) phase and three restarts (warm starts). During the start-up phase of the cold start (approximately the first 15 min of burning) temperature in the combustion chamber was still quite low ($< 400^{o}C$) such that emissions and heat output were highly unstable, whereas combustion became more stable in the second (stable) phase of cold-start burning. Once the system was suitably warmed, a second batch of fuel was loaded into the stove, onto the existing warm charcoal bed and stable burning was achieved more quickly. This process was repeated and then a fourth and final batch was loaded into the stove under conditions intended to simulate poor operation of the appliance. These non-standard combustion conditions were induced by partly closing the air inlet to approximately 25% of the maximum value.

The automatic pellet boiler (LPK 15, Liebi, Switzerland) had a nominal power of 15 kW and was automatically fed with wood pellets (approx. 8 mm in diameter and 15 – 20 mm in

length, moisture content 6.8%). The air was provided and controlled through a two-stage air supply: the primary air supply was injected in the fuel bed while the secondary air supply was injected in the combustion chamber. The combustion cycle consisted of a start-up phase (beginning of burning), a stable burning phase and a poor burning phase (achieved by restricting the air intake).

According to European type-tests (EN303-5), both wood burners were operated with a constant chimney draft of 12 Pa.

Sampling setup and instrumentation. The experimental setup is shown in Figure 1. The exhaust air first passed a heated (150^{o}C) PM_{10} cyclone. After this, a two-stage dilution system was used to deliver the aerosol from the stack of the wood burners to the instruments. The first-stage dilution was performed under heated conditions (150^{o}C), to prevent condensation and particle growth, while the second-stage dilution was performed at room temperature (both VKL 10, Palas, Germany). It should be noted that heated dilution might not be the most suitable for applications regarding health effects of PM as it minimizes the particle partitioning of semivolatile species, which have been identified to play an important role in PM toxicity (*27, 28*). However, it has been adopted as a standard dilution method when sampling combustion aerosols as it produces the most reproducible particle number emission results.

Particle number concentration and particle geometric mean diameter were measured after the dilution systems in real-time (2 s time resolution) using a Diffusion Size Classifier (DiSC; Matter Engineering) (*29*). Particle size distribution was monitored using a Scanning Mobility Particle Sizer (SMPS) consisting of a TSI 3071 Electrostatic Classifier and TSI 3022 Condensation Particle counter. The total mass concentration was measured with a Tapered

Element Oscillating Microbalance (TEOM; Series 1400ab, Thermo Scientific). TEOM data were averaged for each 30 s time period.

An Aerodyne High Resolution Time-of-Flight Aerosol Mass Spectrometer (AMS) was used for the on-line quantification of the submicron non-refractory aerosol components (*30*). The term 'non-refractory' is assigned to those species that evaporate rapidly at 600^{o}C under vacuum conditions. The AMS provided concentrations of particulate organic matter and the average mass spectra for the ensemble of submicron particles (PM_1) with a typical time resolution of 15 s. A particle collection efficiency of the AMS was found to be 1 based on intercomparisons with the other aerosol instrumentation. In this paper, use of AMS data has been limited to quantifying the contribution of the organic fraction to total PM. A detailed analysis of the AMS data will be shown elsewhere.

A thermodenuder (TD; Dekati Ltd.) consisting of a heated tube followed by an activated charcoal section was used to remove semivolatile organic compounds from the particles at a preselected aerosol temperature (250^{o}C). The non-volatile fraction of PM remaining after the TD was monitored by a second DiSC.

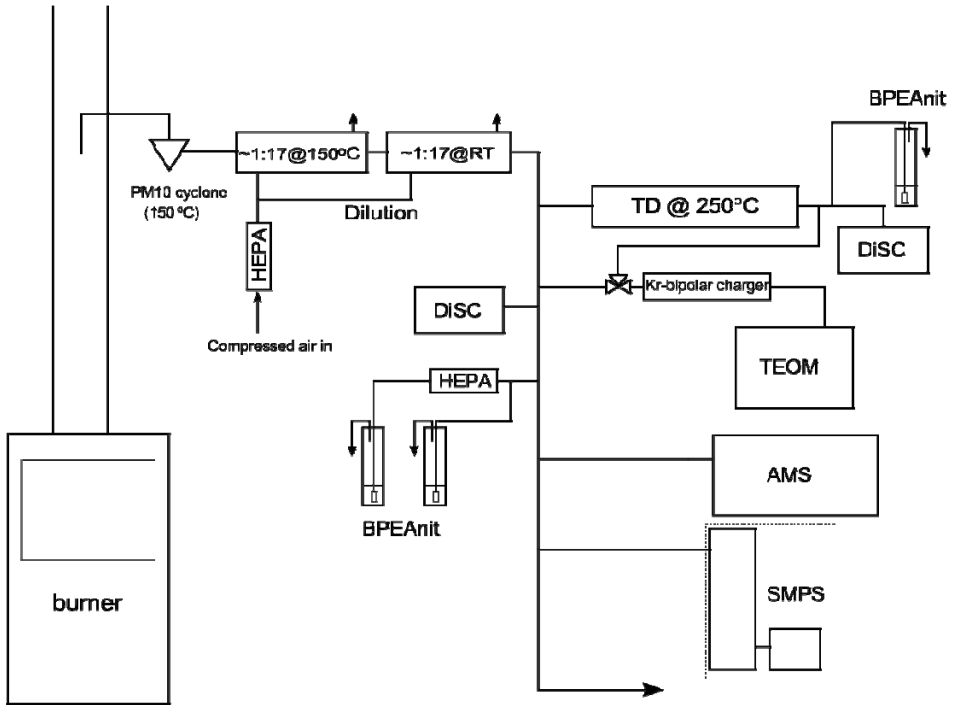

Figure 1. A schematic representation of the experimental setup.

BPEAnit assay. A new profluorescent nitroxide probe, 9-(1,1,3,3-tetramethylisoindolin-2-yloxyl-5-ethynyl)-10-(phenylethynyl)anthracene (BPEAnit) was used to detect ROS in PM produced during biomass combustion. The BPEAnit and its methyl adduct (BPEAnit-Me), which was used for calibration purposes, were synthesised as described previously (*31*). An evaluation of the probe as a means of detecting particle bound ROS has been described previously (*21*). Samples were collected by bubbling aerosol through an impinger containing 20 mL of 4μM BPEAnit solution. Immediately after sampling the fluorescence of the solution was measured. For emissions produced during each of combustion phases, both test and control (HEPA-filtered) samples were collected. In most cases a third sample, taken after the thermodenuder, was also collected. The sampling flow rate was 1 L min^{-1} and the sampling durations were between 10 – 30 min (depending on the combustion phase). A warm-start sampling started approximately 5 minutes after the logs were introduced into the stove, while a poor burning sampling normally began at about 15 minutes after adding the last batch of logwood into the stove. The solvent used in all experiments was ASC grade dimethyl sulfoxide (DMSO; Sigma). Impingers used in this study were custom made and consisted of a Quickfit Dreschel bottle head, with sintered nozzle top (pore size of 100 – 160 μm) and were modified to fit a Quickfit 75 mL test tube (Barloworld Scientific).

Fluorescence measurements. BPEAnit has a fluorescence excitation maximum at 430 nm, and fluorescence emission maxima at 485 and 513 nm. Fluorescence spectra were recorded using a USB2000+ fiber-optic spectrometer combined with a cuvette holder, a pulsed xenon lamp (all Ocean Optics) and a narrow bandpass filter at 430 nm (Edmund Optics). *Calibration curve.* A calibration curve was obtained by plotting known concentrations of fluorescent derivative of BPEAnit (BPEAnit-Me) against the fluorescence intensity at 485 nm. This calibration curve was used to calculate the amount of BPEAnit that was converted

to a fluorescent product when exposed to wood burning PM (assuming that all fluorescence products of BPEAnit have a quantum yield similar to BPEAnit-Me).

Based on the difference of fluorescence signal between the test and control sample, the amount of ROS for each phase was calculated and normalised to the PM mass calculated from the TEOM data.

Results

Particle emissions. Examples of particle emissions from the logwood stove and the automatic pellet boiler in terms of their mass concentration, number concentration and geometric mean diameter ($D_{(GMD)}$) are shown in Figure 2. The graphs show the measured values obtained after dilution and all the reported concentrations are also after dilution. During the cold start (beginning of burning), the mass concentration of particles coming from logwood burning was around 100 µg m^{-3} or lower, with a rapid increase of mass concentration up to several hundred µg m^{-3} upon refilling the stove with logs (Fig. 2A, black). The number concentration for logwood burning particles was between 3×10^4 and 5×10^5 cm^{-3} (Fig. 2 B, black) and the $D_{(GMD)}$ was between 20 and 160 nm (Fig. 2 C, black). Poor burning conditions were induced by reducing the intake air approximately 15 min after loading the last batch of logs into the stove. Interestingly, this resulted in a substantial decrease in particle number and mass. Reducing the air intake reduces the air flow into the stack from the combustion chamber. This might be the reason for the observed decrease in particle number and mass concentrations.

Particle emissions coming from the automatic pellet boiler resulted in a strong and sharp peak in mass concentration at the beginning of burning (start-up) reaching up to 2200 µg m^{-3}. During stable burning, the particle mass concentration was around 100 µg m^{-3}, becoming less stable and 2-3 times higher during poor burning (Fig. 2 A, grey). Particle number

concentration and $D_{(GMD)}$ during stable burning were around 2.2×10^5 cm^{-3} and 100 nm, respectively, and were quite uniform during this phase. During poor burning, both particle number concentration and diameter varied significantly with the number concentration in the range of 2×10^5 and 6×10^5 cm^{-3}, and the $D_{(GMD)}$ varying between 90 and 170 nm (Fig. 2 B and C, grey).

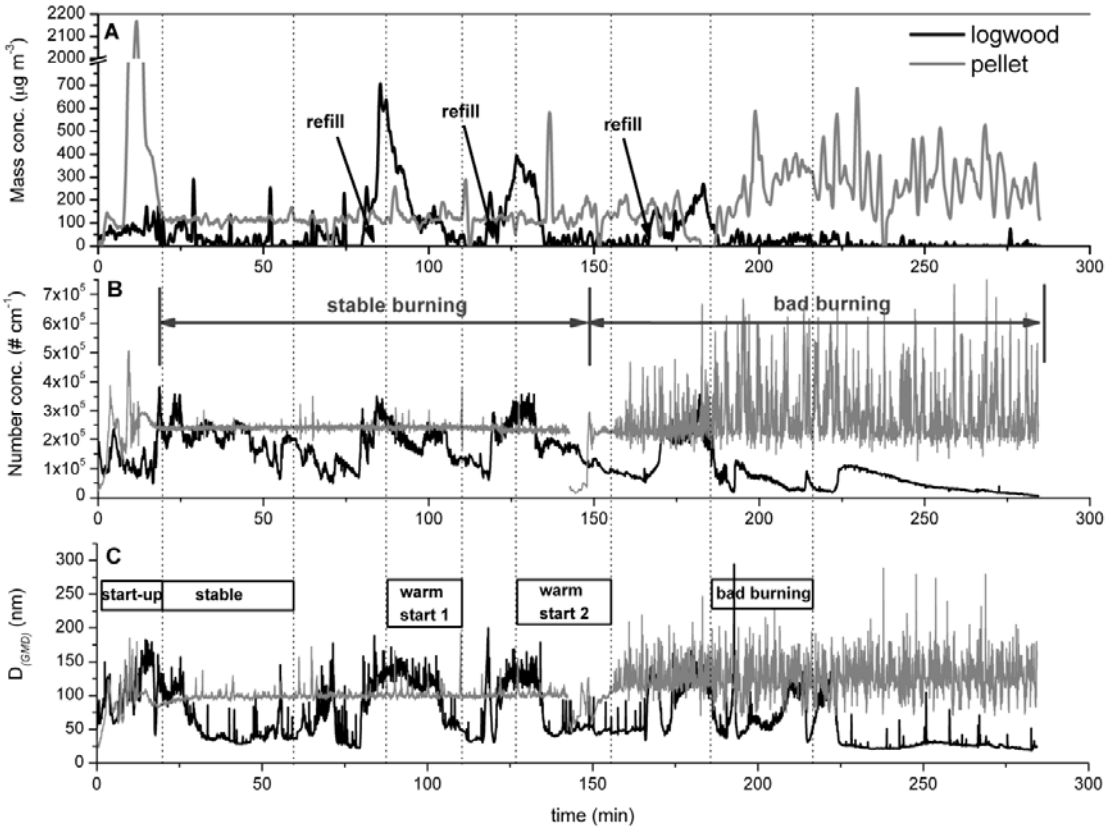

Figure 2. Examples of mass concentration (A), number concentration (B) and geometric mean diameter ($D_{(GMD)}$; C) for particles from logwood burning in the traditional logwood stove (black) and the automatic pellet boiler (grey). The graphs show the values after dilution. Dotted lines denote the time periods at which samples for each phase of logwood burning were normally taken.

ROS from logwood burning particles. The amount of BPEAnit being converted to a fluorescent product was normalized with respect to PM mass (as measured by the TEOM) providing a measure of ROS concentration. Given that the collection efficiency of impingers

is less than 100%, a correction for mass loss during sampling was required (for details on the procedure see Supporting Information).

Figure 3 shows average ROS concentrations for cold and warm-start logwood burning particles. It can be seen that the cold-start phase resulted in much higher ROS concentrations than the warm-start phase, especially during the stable burning phase. ROS concentrations related to particle emissions from the stable phase of the cold start (4000 ± 260 nmol mg^{-3}) were about 3 times higher than ROS concentrations from start-up phase of cold start (1230 ± 100 nmol mg^{-3}), and about 9 -18 times higher than the ROS concentrations from the warm-start burning (450 ± 250 nmol mg^{-3} and 220 ± 50 nmol mg^{-3}) phases. ROS concentrations for poor burning are not shown in the graph as they resulted in large variations between repeats (0 – 3100 nmol mg^{-1}).

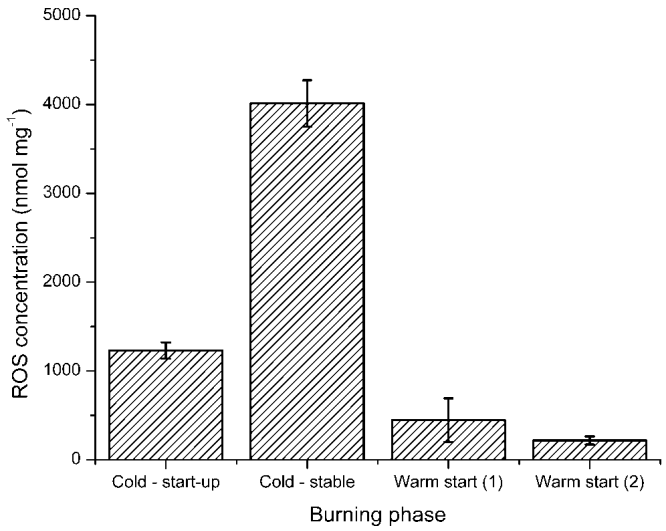

Figure 3. Average ROS concentrations of logwood burning particle emissions for cold and warm start. Warm start 1 and 2 present sampling after refilling the stove for the first and second time. Error bars present one standard error (n=4).

Correlation between ROS and organics. In addition to control and test samples, in most of the cases a third sample, collected after passing the aerosol through the thermodenuder (TD), was also obtained. The purpose of the TD was to remove semivolatile organics condensed onto particles. The particles from logwood burning showed a significant reduction (85 – 100%) of fluorescence emission of BPEAnit after the TD compared to the particles that had not passed through the TD. Figure 4 shows the fluorescence intensity of BPEAnit from two samples taken simultaneously, one with and one without the TD placed in front of it. The fact that sampling after the TD results in very small or no increase of BPEAnit fluorescence compared to the baseline fluorescence (Figure 4; black curve) indicates the role of semivolatile organic species condensed in the oxidative capacity of PM.

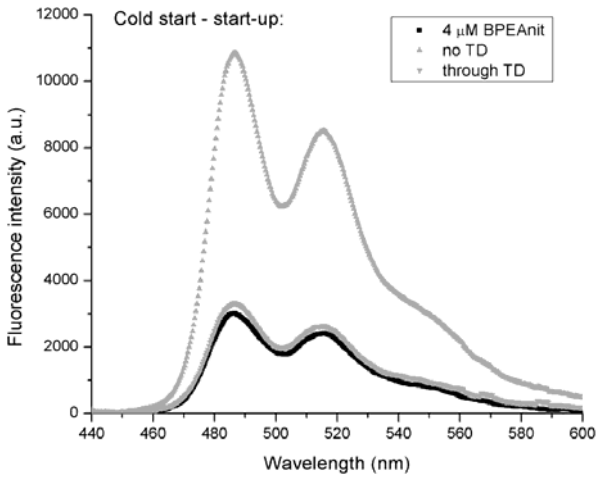

Figure 4. Fluorescence emission of BPEAnit when sampling with and without a thermodenuder.

The role of the volatile organic fraction was further investigated by plotting for each sample the amount of ROS against the amount of organics (Figure 5). The amount of organic material was calculated by integrating the mass concentration of organics as measured by the AMS over the sampling time and multiplying by the sampling flow rate of the impinger

setup. Considering the large differences in ROS concentrations for each burning phase (see Figure 3), a correlation between ROS and organics is presented for each phase separately in Figure 5. Results for the warm-start phase 1 and 2 are plotted on the same graph (Figure 5. C), as the difference in their ROS concentrations is not statistically significant. While there is a rather weak correlation between ROS and organics for the start-up phase of the cold start (Figure 5. A), ROS and organics for the stable phase of the cold start (Figure 5. B) and especially for the warm start (Figure 5. C) show a strong correlation (r = 0.850 and 0.989, respectively, where r is the Pearson correlation coefficient). It is important to note that, while the scale on the y-axis is the same, the scale on the x-axis is not, and the difference in the slopes for Figure 5 B and C (see equations in the Figures) indicates the difference in the reactivity of the organic species related to these burning phases, with organics from the stable phase of the cold start being much more reactive than organics from warm-start burning. It is difficult to draw conclusions for the start-up phase of cold start due to the weak correlation and limited number of data points.

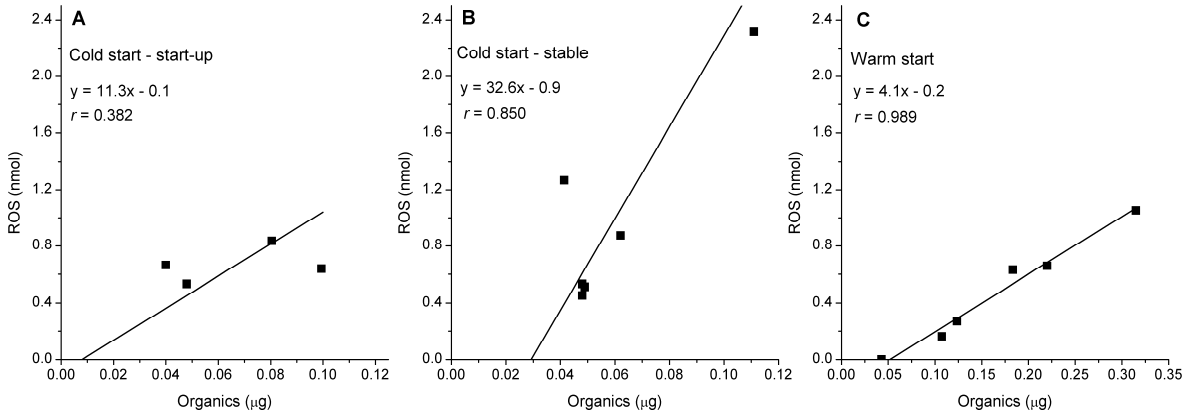

Figure 5. Correlation between the amount of ROS and the amount of organics for start-up phase of cold-start (A), stable phase of cold-start (B) and warm-start (C) logwood burning.

ROS from pellet burning particles. Figure 6 shows the fluorescence intensity of BPEAnit after sampling emissions coming from the automatic pellet boiler. The fluorescence intensity of both the control (HEPA-filtered) and the test sample are slightly higher than the baseline fluorescence intensity of BPEAnit (i.e. fluorescence intensity prior to sampling), but there is no difference in fluorescence intensity between the control and the test sample, indicating that particles from combustion in the automatic pellet boiler do not contain detectable levels of ROS or other redox active species. The example shown in the Figure 6 is for the beginning of the burning (start-up), the same result was observed for stable and poor burning, and also observed for prolonged sampling periods (~1h).

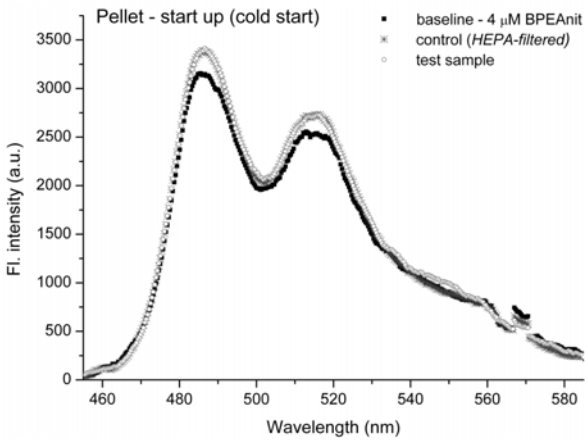

Figure 6. Fluorescence intensity of BPEAnit after sampling emissions from the automatic pellet boiler.

Discussion

In this study we show that particulate emissions produced by a traditional logwood stove induce an increase in fluorescence of BPEAnit, indicating the presence of ROS and other redox active species in these particles. On the other hand, particles produced by the automatic pellet boiler did not induce an increase in BPEAnit fluorescence. This indicates that within

the detection limit of this method there are no ROS present in these particles and suggests that particulate emissions from pellet boilers have a lower toxicological potential than emissions from logwood stoves. One of the reasons for these observations might be the different combustion temperature. The temperature of the combustion chamber in the automatic pellet boiler was around 1050^{o}C during stable burning and around 950^{o}C during poor burning, while the temperatures in the combustion chamber of the traditional logwood stove peaked at 650 – 750^{o}C (Figure S2 in Supporting Information). Also, during the cold start of logwood burning, the maximum temperature in the combustion chamber was substantially lower (400 – 500^{o}C) than during the warm-start burning (650 – 750^{o}C). This might be the reason why cold-start emissions resulted in much higher ROS concentrations than the warm-start emissions. A similar trend in ROS concentrations was observed by Surawski et al. (*20*), who found that ROS concentrations related to diesel PM tend to decrease as the engine load and subsequently the combustion temperature increases.

Interestingly, particles produced during the start-up phase of the cold start had 3 times lower ROS per PM mass than the stable phase of the cold start. This was observed even though the temperature in the combustion chamber during the start-up was lower than the temperature during stable burning. We infer that this discrepancy between our previously stated hypothesis and the start-up phase of cold start is an artefact incurred by the dilution system. Given that start-up flue gas temperatures during the first 15 min averaged 80^{o}C while first-stage dilution temperature was 150^{o}C, it is likely that a significant fraction of any semivolatile species were volatilised during the first-stage dilution process. The flue gas temperature for all other burning phases was higher than 150^{o}C. So evaporation of semivolatile species during dilution might be an explanation for the lower ROS concentration observed start-up phase of cold start than for cold-start stable burning.

ROS concentrations were plotted against the logwood combustion chamber temperature averaged for each sampling interval and, as shown in Figure 7, a strong negative correlation (r = -0.876) is obtained. This supports our hypothesis that higher temperature of the combustion chamber will result in lower ROS concentrations. It is important to mention that due to the aforementioned differences between the flue gas and the dilution temperature, ROS concentrations obtained for the start-up phase of cold-start burning were excluded from the Figure.

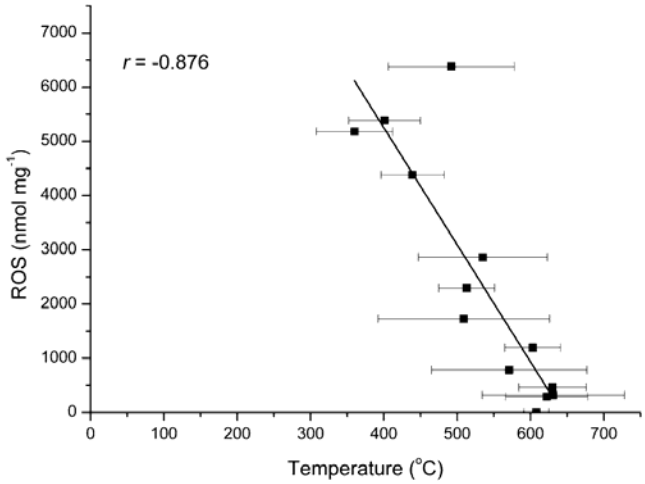

Figure 7. Correlation between the combustion chamber temperature and ROS concentration for logwood burning. Error bars present one standard deviation.

Another important observation from this study is the 80 – 100% reduction of BPEAnit fluorescence intensity when the volatile fraction of the logwood burning particles is removed by a thermodenuder at 250^{o}C. This suggests that ROS observed during our measurements are related to the volatile (i.e. organic) components of the PM. A significant reduction in PM oxidative potential after thermal conditioning was also observed by Biswas and co-workers (*27*) who used a dithiothreitol (DTT) assay to measure the oxidative potential of particulate matter produced by heavy–duty vehicles. As a further support of the role of organic species in

particle induced oxidative stress, we observed strong correlations (r = 0.85 and 0.99) between the amount of ROS and the mass fraction of organic species in the PM during cold-start stable combustion and warm-start combustion (Figure 5 B and C). Also, it should be noted that the x-axis scales in Figure 5 B and C are not equal and that the slope of the fitted curve for stable phase of the cold-start (Figure 5 B) is about 8 times higher than the warm-start burning slope (Figure 5 C). This difference in the slopes suggests that there is a difference in the reactivity or in the abundance of reactive species between organic fractions of particles coming from cold and warm-start burning.

In previous studies involving the BPEAnit assay employed here the oxidative potential of particles in cigarette smoke and diesel exhaust was investigated (*20, 21*). In comparison with this study, particles from sidestream cigarette smoke (*21*) have 4-9 and 30-80 times less ROS per unit of mass than particles produced during warm-start and cold-start logwood combustion, respectively. Diesel exhaust particles generated under full engine load were found to have similar ROS concentrations as sidestream cigarette smoke particles (~50 nmol mg^{-1}) (*20*). On the other hand, diesel exhaust particles generated during idling were found to have ROS concentrations similar to those observed for stable phase of cold-start logwood burning. The main difference between diesel exhaust particles generated under full engine load and during idling was in the occurrence of the nucleation mode during idling. While diesel exhaust PM generated under full engine load consisted only of accumulation mode, the important feature of the size distribution for PM generated during engine idling was a strong nucleation mode occurrence and a reduction in the accumulation mode particle concentration. Nucleation mode particles contribute very little to PM mass and are composed mainly of organic (semivolatile) species. The significant increase of ROS concentration for particles generated during idling was associated with the semivolatile species present in the nucleation mode. In this study we have observed a decrease of the ROS concentration upon removal of

the semivolatile species. Both studies indicate a strong link between semivolatile species and ROS and therefore the importance of semivolatiles in the oxidative potential of the particulate matter.

Acknowledgments

This work was supported by the Swiss Federal Office of Energy and the Swiss Federal Office for the Environment, the IMBALANCE project of the Competence Center Environment and Sustainability of the ETH Domain (CCES) and the ARC Centres of Excellence Program CEO 0561607. BM would like to thank the EC project EUROCHAMP for the travel support and financial support during the campaign. PFD is grateful for support from the US-NSF (IRFP #0701013).

References

1. Glasius, M.; Ketzel, M.; Wåhlin, P.; Jensen, B.; Mønster, J.; Berkowicz, R.; Palmgren, F. Impact of wood combustion on particle levels in a residential area in Denmark. *Atmos. Environ.* **2006,** *40* (37), 7115-7124.

2. Szidat, S.; Prevot, A. S. H.; Sandradewi, J.; Alfarra, M. R.; Synal, H. A.; Wacker, L.; Baltensperger, U. Dominant impact of residential wood burning on particulate matter in Alpine valleys during winter. *Geophys. Res. Lett.* **2007,** *34* (5), 1-6.

3. de Kok, T. M. C. M.; Driece, H. A. L.; Hogervorst, J. G. F.; Briede, J. J. Toxicological assessment of ambient and traffic-related particulate matter: A review of recent studies. *Mut. Res./Rev. Mut. Res.* **2006,** *613* (2-3), 103-122.

4. Pope, C. A.; Burnett, R. T.; Thun, M. J.; Calle, E. E.; Krewski, D.; Ito, K.; Thurston, G. D. Lung cancer, cardiopulmonary mortality, and long-term exposure to fine particulate air pollution. *J. Am. Med. Assoc.* **2002,** *287*, 1132 - 1141.

5. Danielsen, P. H.; Loft, S.; Kocbach, A.; Schwarze, P. E.; Møller, P. Oxidative damage to DNA and repair induced by Norwegian wood smoke particles in human A549 and THP-1 cell lines. *Mut. Res./Gen. Toxicol. Environ. Mut.* **2009,** *674* (1-2), 116-122.

6. Kocbach, A.; Namork, E.; Schwarze, P. E. Pro-inflammatory potential of wood smoke and traffic-derived particles in a monocytic cell line. *Toxicol.* **2008,** *247* (2-3), 123-132.

7. Leonard, S. S.; Castranova, V.; Chen, B. T.; Schwegler-Berry, D.; Hoover, M.; Piacitelli, C.; Gaughan, D. M. Particle size-dependent radical generation from wildland fire smoke. *Toxicol.* **2007,** *236* (1-2), 103-113.

8. Leonard, S. S.; Wang, S. W.; Shi, X. L.; Jordan, B. S.; Castranova, V.; Dubick, M. A. Wood smoke particles generate free radicals and cause lipid peroxidation, DNA damage, NF kappa B activation and TNF-alpha release in macrophages. *Toxicol.* **2000,** *150* (1-3), 147-157.

9. Naeher, L. P.; Brauer, M.; Lipsett, M.; Zelikoff, J. T.; Simpson, C. D.; Koenig, J. Q.; Smith, K. R. Woodsmoke health effects: A review. *Inhal. Toxicol.* **2007,** *19* (1), 67-106.

10. Kocbach, A.; Namork, E.; Schwarze, P. E. Pro-inflammatory potential of wood smoke and traffic-derived particles in a monocytic cell line. *Toxicol.* **2008,** *247*, 123 - 132.

11. Kocbach Bolling, A.; Pagels, J.; Yttri, K.; Barregard, L.; Sallsten, G.; Schwarze, P.; Boman, C. Health effects of residential wood smoke particles: the importance of combustion conditions and physicochemical particle properties. *Part. Fibre. Toxicol.* **2009,** *6* (1), 29.

12. Nel, A. ATMOSPHERE: Enhanced: Air pollution-related illness: Effects of particles. *Science* **2005,** *308* (5723), 804-806.

13. Tao, F.; Gonzalez-Flecha, B.; Kobzik, L. Reactive oxygen species in pulmonary inflammation by ambient particulates. *Free Radical Biol. Med.* **2003,** *35* (4), 327-340.

14. Hung, H. F.; Wang, C. S. Experimental determination of reactive oxygen species in Taipei aerosols. *J. Aerosol Sci.* **2001,** *32* (10), 1201-1211.

15. Venkatachari, P.; Hopke, P. K.; Brune, W. H.; Ren, X. R.; Lesher, R.; Mao, J. Q.; Mitchel, M. Characterization of wintertime reactive oxygen species concentrations in Flushing, New York. *Aerosol Sci. Technol.* **2007,** *41* (2), 97-111.

16. Venkatachari, P.; Hopke, P. K.; Grover, B. D.; Eatough, D. J. Measurement of particle-bound reactive oxygen species in Rubidoux aerosols. *J. Atmos. Chem.* **2005,** *50* (1), 49-58.

17. Jia, M.; Tang, Y.; Lam, Y.-F.; Green, S. A.; Blough, N. V. Prefluorescent nitroxide probe for the highly sensitive determination of peroxyl and other radical oxidants. *Anal. Chem.* **2009,** *81* (19), 8033-8040.

18. Micallef, A. S.; Blinco, J. P.; George, G. A.; Reid, D. A.; Rizzardo, E.; Thang, S. H.; Bottle, S. E. The application of a novel profluorescent nitroxide to monitor thermo-oxidative degradation of polypropylene. *Polym. Degrad. Stab.* **2005,** *89* (3), 427-435.

19. Pou, S.; Huang, Y. I.; Bhan, A.; Bhadti, V. S.; Hosmane, R. S.; Wu, S. Y.; Cao, G. L.; Rosen, G. M. A fluorophore-containing nitroxide as a probe to detect superoxide and hydroxyl radical generated by stimulated neutrophils. *Anal. Biochem.* **1993,** *212* (1), 85-90.

20. Surawski, N. C.; Miljevic, B.; Roberts, B. A.; Modini, R. L.; Situ, R.; Brown, R. J.; Bottle, S. E.; Ristovski, Z. D. Particle emissions, volatility and toxicity from an ethanol fumigated compression ignition engine. *Environ. Sci. Technol.* **2009,** *44* (1), 229-235.

21. Miljevic, B.; Fairfull-Smith, K. E.; Bottle, S. E.; Ristovski, Z. D. The application of profluorescent nitroxides to detect reactive oxygen species derived from combustion-

generated particulate matter: Cigarette smoke - A case study. *Atmos. Environ.* **2010,** *44* (18), 2224-2230.

22. Johansson, L. S.; Leckner, B.; Gustavsson, L.; Cooper, D.; Tullin, C.; Potter, A. Emission characteristics of modern and old-type residential boilers fired with wood logs and wood pellets. *Atmos. Environ.* **2004,** *38* (25), 4183-4195.

23. Oser, M.; Nussbaumer, T.; Schweizer, B.; Mohr, M.; Figi, R. Influence on aerosol formation in an automatic wood furnace. *Proceedings of the International Seminar of IEA Bioenergy Task 32: Aerosols from Biomass Combustion* **2001**, 59-64.

24. Rau, J. A. Composition and Size Distribution of Residential Wood Smoke Particles. *Aerosol Sci. Technol.* **1989,** *10* (1), 181 - 192.

25. Schmidl, C.; Marr, I. L.; Caseiro, A.; Kotianová, P.; Berner, A.; Bauer, H.; Kasper-Giebl, A.; Puxbaum, H. Chemical characterisation of fine particle emissions from wood stove combustion of common woods growing in mid-European Alpine regions. *Atmos. Environ.* **2008,** *42* (1), 126-141.

26. Nussbaumer, T.; Czasch, C.; Klippel, N.; Johansson, L.; Tullin, C. *Particulate emissions from biomass combustion in IEA countries: Survey on measurements and emission factors*; International Energy Agency (IEA) Bioenergy Task 32 and Swiss Federal Office of Energy (SFOE): Zurich, 2008.

27. Biswas, S.; Verma, V.; Schauer, J. J.; Cassee, F. R.; Cho, A. K.; Sioutas, C. Oxidative potential of semi-volatile and non volatile particulate matter (PM) from heavy-duty vehicles retrofitted with emission control technologies. *Environ. Sci. Technol.* **2009,** *43* (10), 3905-3912.

28. Li, N.; Wang, M. Y.; Oberley, T. D.; Sempf, J. M.; Nel, A. E. Comparison of the pro-oxidative and proinflammatory effects of organic diesel exhaust particle chemicals in bronchial epithelial cells and macrophages. *J. Immunol.* **2002,** *169* (8), 4531-4541.

29. Fierz, M.; Burtscher, H.; Steigmeier, P.; Kasper, M. Field measurement of particle size and number concentration with the Diffusion Size Classifier (DiSC). *SAE* **2008**, 2008-01-1179.

30. DeCarlo, P. F.; Kimmel, J. R.; Trimborn, A.; Northway, M. J.; Jayne, J. T.; Aiken, A. C.; Gonin, M.; Fuhrer, K.; Horvath, T.; Docherty, K. S.; Worsnop, D. R.; Jimenez, J. L. Field-deployable, high-resolution, time-of-flight aerosol mass spectrometer. *Anal. Chem.* **2006,** *78* (24), 8281-8289.

31. Fairfull-Smith, K. E.; Bottle, S. E. The synthesis and physical properties of novel polyaromatic profluorescent isoindoline nitroxide probes. *Eur. J. Org. Chem.* **2008,** *32*, 5391-5400.

Brief

As measured by the novel BPEAnit assay, logwood burning particles have substantially higher oxidative stress potential than pellet burning particles, especially during cold start burning phase.